DOI: 10.1002/chem.201002135

High Gas Sorption and Metal-Ion Exchange of Microporous Metal–Organic Frameworks with Incorporated Imide Groups

Thazhe Kootteri Prasad, Dae Ho Hong, and Myunghyun Paik Suh*[a]

Abstract: Metal–organic frameworks (MOFs), $\{[Cu_2(bdcppi)(dmf)_2]\cdot 10DMF\cdot 2H_2O\}_n$ (SNU-50) and $\{[Zn_2(bdcppi)(dmf)_3]\cdot 6DMF\cdot 4H_2O\}_n$ (SNU-51), have been prepared by the solvothermal reactions of *N*,*N*′-bis(3,5-dicarboxyphenyl)pyromellitic diimide (H_4BDCPPI) with $Cu(NO_3)_2$ and $Zn(NO_3)_2$, respectively. Framework SNU-50 has an NbO-type net structure, whereas SNU-51 has a PtS-type net structure. Desolvated solid $[Cu_2(bdcppi)]_n$ (SNU-50′), which was prepared by guest exchange of SNU-50 with acetone followed by evacuation at 170 °C, adsorbs high amounts of N_2, H_2, O_2, CO_2, and CH_4 gases due to the presence of a vacant coordination site at every metal ion, and to the presence of imide groups in the ligand. The Langmuir surface area is 2450 $m^2 g^{-1}$. It adsorbs H_2 gas up to 2.10 wt% at 1 atm and 77 K, with zero coverage isosteric heat of 7.1 kJ mol^{-1}, up to a total of 7.85 wt% at 77 K and 60 bar. Its CO_2 and CH_4 adsorption capacities at 298 K are 77 wt% at 55 bar and 17 wt% at 60 bar, respectively. Of particular note is the O_2 adsorption capacity of SNU-50′ (118 wt% at 77 K and 0.2 atm), which is the highest reported so far for any MOF. By metal-ion exchange of SNU-51 with Cu^{II}, $\{[Cu_2(bdcppi)(dmf)_3]\cdot 7DMF\cdot 5H_2O\}_n$ (SNU-51-Cu_{DMF}) with a PtS-type net was prepared, which could not be synthesized by a direct solvothermal reaction.

Keywords: gas adsorption · hydrogen storage · metal–organic frameworks · microporous materials · oxygen

Introduction

Metal–organic frameworks (MOFs) with pores and channels have attracted great attention because of their potential applications in gas storage, gas separation, catalysis, and fabrication of nanoparticles.[1–4] The storage of H_2 and CH_4 gases and the capture of CO_2 have become particularly important issues in MOF chemistry, because of the potential utility of H_2 and CH_4 as energy carriers, and the implications of CO_2 in global warming. There are a number of MOFs that adsorb high levels of CO_2[4] and CH_4[5–7] at room temperature, but their H_2 storage capacities[1,3,8–10] are generally very low at room temperature because of the low isosteric heat of H_2 adsorption. The isosteric heat of H_2 adsorption can be increased by the creation of open metal sites, through synthesis of catenated frameworks, and by imbedding metal nanoparticles in the MOF.[1,2f,3] Gas sorption properties also depend on pore volume and ligand structures. It has been reported that curved ligands incorporated into a MOF can increase H_2 adsorption because they provide a pocket for adsorption.[11]

Various MOFs have been constructed from Cu^{II} and tetracarboxylic acids,[3,5,6,8,11,12] some of which are reported to show high H_2 adsorption capacities,[3,8,11,12a] but sorption properties for other gases have been less well explored.[6] In addition, the tetracarboxylate ligands used in the previous studies did not contain extra functional groups. This has prompted us to synthesize MOFs in which the organic ligand incorporates imide groups, and to explore their effects on gas sorption. In addition, several recent reports show that the properties of MOFs can be altered by using postsynthetic modifications, such as covalent transformations, tandem modifications, protonation, and doping with metals.[13] It has been also reported that the coordinated metal ions in the MOF can be reversibly exchanged while maintaining structural integrity.[14]

In this work, we have prepared a new ligand *N*,*N*′-bis(3,5-dicarboxyphenyl)pyromellitic diimide (H_4BDCPPI). We ex-

[a] Dr. T. K. Prasad, D. H. Hong, Prof. M. P. Suh
Department of Chemistry, Seoul National University
Seoul 151-747 (Republic of Korea)
Fax: (+82) 28868516
E-mail: mpsuh@snu.ac.kr

Supporting information for this article is available on the WWW under http://dx.doi.org/10.1002/chem.201002135 or from the author. It includes general methods, additional views of the crystal structures, TGA, PXRD patterns, and technical details of adsorption measurements.

pected that the imide groups might influence the gas sorption properties. By employing this long tetracarboxylate ligand, we synthesized $\{[Cu_2(bdcppi)(dmf)_2]\cdot 10DMF\cdot 2H_2O\}_n$ (SNU-50) and $\{[Zn_2(bdcppi)(dmf)_3]\cdot 6DMF\cdot 4H_2O\}_n$ (SNU-51), which have entirely different structures; namely, NbO-type and PtS-type net structures, respectively (see Scheme 1). The desolvated solid $[Cu_2(bdcppi)]_n$ (SNU-50′)

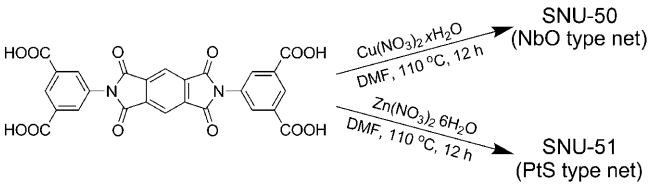

Scheme 1. Construction of porous networks by using *N*,*N*′-bis(3,5-dicarboxyphenyl)pyromellitic diimide (H_4BDCPPI).

exhibits high adsorption capacities for N_2, H_2, O_2, CO_2, and CH_4 gases, which must be attributed to the presence of the vacant coordination site at every metal ion and the presence of imide groups in the ligand. The Zn^{II} ions in SNU-51 were exchanged with Cu^{II} ions with retention of the PtS-type net—a structure that was impossible to prepare through solvothermal reaction.

Results and Discussion

Synthesis and X-ray structure of SNU-50: Bluish green crystals of SNU-50 were prepared by heating an acidified mixture of $Cu(NO_3)_2$ and H_4BDCPPI in DMF at 110 °C for 12 h. The X-ray crystal structure of SNU-50 indicates that the Cu^{II} ions form a paddlewheel-type $[Cu_2(OOC)_4]$ cluster as a square-planar secondary building unit (SBU) that is linked with the rectangular organic building block $BDCPPI^{4-}$ to give rise to a NbO-type 3D network (see Figure 1). Each Cu^{II} ion shows square pyramidal geometry, with the coordination of four oxygen atoms from four different $BDCPPI^{4-}$ units and a DMF molecule coordinated at the axial position of the paddlewheel unit.

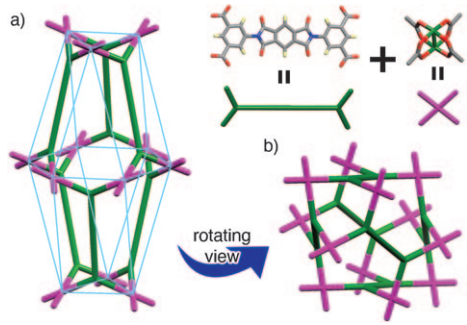

Figure 1. X-ray crystal structure of SNU-50. a) View showing a barrel-like cage that consists of $Cu_{24}(BDCPPI)_6$. Color scheme: $[Cu_2(OOC)_4]$ paddlewheel units = purple, BDCPPI ligand = green. b) Simplified view showing the NbO-type net.

The framework creates barrel-like cages, each of which is composed of 12 nodes occupied by $[Cu_2(OOC)_4]$ cluster units (see Figure 1 a). The edge length of the external triangular ring of the cage is about 10 Å, as estimated from the centers of the paddlewheel units, while the diagonal distance for the internal hexagonal ring is about 28 Å. Because of the long organic linker, a huge void space is created in the lattice. The void volume of SNU-50 calculated by PLATON is 63 % of the unit-cell volume without any guest molecules, and it increases to 74 % upon removal of the coordinated DMF molecules. The framework contains three types of channels, two of which are similar. The cylindrical channel with an aperture diameter of 3 Å passes along the *c* axis of the unit cell. The two similar channels, with maximum in-circle diameters of 2.0 Å, pass along the *a* and *b* axes of the unit cell (see Figure S2 in the Supporting Information). The channels are filled with DMF and H_2O guest molecules. Because the guest solvent molecules could not be located from the difference map due to their high thermal disorder in the large unit cells, the identity and numbers of guest molecules were determined from elemental analysis (EA) and thermogravimetric analysis (TGA) data. The channel size increases upon removal of the coordinated DMF molecules; the channel along the *c* axis increases to 4 Å, while the channels along the *a* and *b* axes change to triangular type with maximum in-circle diameters of 4.5 Å (see Figure S2 in the Supporting Information). TGA of SNU-50 indicates that the coordinated DMF molecules can be removed at 220 °C, and the framework is stable up to 290 °C (see Figure S5 in the Supporting Information).

When SNU-50 was immersed in anhydrous acetone, the coordinated DMF molecules and the guest solvent molecules were exchanged with acetone to produce $\{[Cu_2(bdcppi)(CH_3COCH_3)_2]\cdot 5CH_3COCH_3\cdot 2H_2O\}_n$ ($SNU\text{-}50_{Ac}$). $SNU\text{-}50_{Ac}$ was characterized by IR, EA, and TGA. The coordinated acetone at the Cu^{II} ion could be clearly seen at 1689 cm^{-1} in the IR spectra. A few X-ray structures have been reported for acetone-coordinated complexes.[15] Although the single-crystal X-ray structure of $SNU\text{-}50_{Ac}$ could not be determined because of the poor diffraction profile, the powder XRD (PXRD) pattern indicated that the framework structure changed very little with guest exchange (see Figure S7 in the Supporting Information).

Gas sorption of SNU-50′: The preparation of SNU-50′ was achieved by heating $SNU\text{-}50_{Ac}$ at 60 °C for 24 h and then at 170 °C for 4 h. The structure of SNU-50′ contains a vacant coordination site at every Cu^{II} ion, and is extremely moisture sensitive; its dark blue color changes instantly to pale green on exposure to air, and its PXRD pattern becomes broadened, although the peak positions are similar to those of SNU-50 and $SNU\text{-}50_{Ac}$ (see Figure S7 in the Supporting Information). Once SNU-50′ is exposed to air, it does not adsorb any gases even after it is reactivated.

The permanent porosity of SNU-50′ was confirmed by the adsorption isotherms of N_2, H_2, O_2, CO_2, and CH_4 gases (see Figure 2 and Table 1). The N_2 adsorption isotherm at 77 K

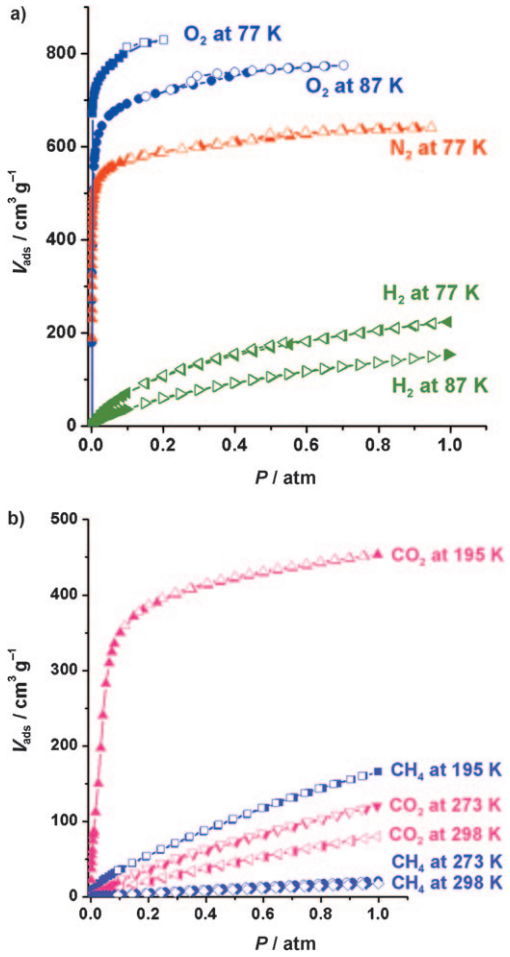

Figure 2. Gas adsorption isotherms of SNU-50′ for a) H_2, N_2, and O_2 at 77 K and 87 K, and b) CO_2 and CH_4 at 195 K, 273 K, and 298 K. Filled shapes = adsorption, open shapes = desorption.

Table 1. Gas adsorption data for SNU-50′.

Gas	T [K]	P [bar]	V_{ads} [cm^3 g^{-1}]	Amount [mmol g^{-1}]	Amount [wt %]
N_2	77	0.9	641	28.6	80.1
H_2	77	1.0	233	10.4	2.10
	87	1.0	154	6.88	1.39
	77	60	614,[a] 913[b]	27.4,[a] 39.0[b]	5.53,[a] 7.86[b]
	298	61	44.4,[a] 119[b]	1.98,[a] 4.86[b]	0.399,[a] 0.980[b]
O_2	77	0.20	829	37.0	118
	87	0.70	774	34.6	110
CO_2	195	1.0	454	20.3	89.3
	273	1.0	120	5.36	23.6
	298	1.0	80	3.6	16
	298	46	383	17.1	75.2
CH_4	195	1.0	166	7.41	11.9
	273	1.0	21	0.94	1.5
	298	1.0	17	0.76	1.2
	298	61	237	10.6	17.0

[a] Excess adsorption capacity. [b] Total adsorption capacity.

shows Type-I sorption behavior, which is characteristic of microporosity. SNU-50′ adsorbs 641 cm^3 g^{-1} of N_2 at 77 K and 0.89 atm. The Brunauer–Emmett–Teller (BET) and Langmuir surface areas are 2300 and 2450 m^2 g^{-1}, respectively, which are smaller than the accessible surface area (3455 m^2 g^{-1}) calculated for SNU-50 by simple Monte Carlo simulation with N_2 as a probe molecule (probe diameter = 3.681 Å).[16] The pore volume calculated by using the Dubinin–Radushkevich method was 1.08 cm^3 g^{-1}, which is slightly smaller than the value (1.11 cm^3 g^{-1}) calculated from the X-ray crystal structure of SNU-50 by using PLATON.[17] The reduced surface area and pore volume, compared with those of the theoretical values, indicate that the framework shrinks on removal of the coordinated solvent molecules as well as the guest molecules. The pore diameter calculated with the Saito–Foley model[18] was 11.0 Å (see the Supporting Information). The density of N_2 adsorbed in SNU-50′, as calculated by using the pore volume (1.08 cm^3 g^{-1}) estimated from the N_2 adsorption data, is 743 kg m^{-3}, which is close to the liquid N_2 density of 807 kg m^{-3} at 77 K and 1 atm.

The H_2 adsorption isotherms measured at 77 and 87 K show the high H_2 uptake capability of SNU-50′. It adsorbs up to 2.10 wt % of H_2 (233 cm^3 g^{-1} at standard temperature and pressure (STP), 6.9 H_2 molecules per formula unit) at 77 K and 1 atm, and up to 1.39 wt % (154 cm^3 g^{-1} at STP, 4.5 H_2 molecules per formula unit) at 87 K and 1 atm. The isosteric heat of H_2 adsorption calculated by using the virial equation[10b,19] is 7.1–4.7 kJ mol^{-1}, depending on the amount of H_2 uptake (see Figure S12 in the Supporting Information). The values are comparable with those of previously reported Cu^{II} MOFs that contain the accessible metal sites on Cu^{II} and the long tetracarboxylate ligand.[3,8,11] The density of adsorbed H_2 in SNU-50′ at 77 K and 1 atm, as calculated by using the pore volume (1.08 cm^3 g^{-1}) estimated from the N_2 adsorption data, is 19 kg m^{-3}, which is much lower than that of liquid H_2 (71 kg m^{-3} at 1 atm and 20 K).

The O_2 gas adsorption isotherm of SNU-50′ was measured up to 0.20 atm because the saturation pressure of O_2 at 77 K is 147.8 Torr. SNU-50′ adsorbs 829 cm^3 g^{-1} (118 wt %) of O_2 at 77 K and 0.20 atm, and 774 cm^3 g^{-1} (110 wt %) at 87 K and 0.7 atm. These values are the highest yet observed for any MOF. Previously, the highest adsorption data reported for O_2 was 618 cm^3 g^{-1} (88 wt %) at 77 K and 0.19 atm for Co(BDP).[20] In addition, SNU-50′ adsorbs much higher amounts (1.5×) of O_2 than N_2 at 77 K and 0.2 atm. This may be attributed to the fact that the vacant coordination sites on the Cu^{II} centers of the framework interact with O_2 more strongly than with N_2.[21] In addition, O_2 is more accessible to the channels with smaller apertures because of its smaller kinetic diameter (3.47 Å) than that of N_2 (3.64 Å). The density of adsorbed O_2 in the framework, as calculated by using the pore volume (1.08 cm^3 g^{-1}) estimated from the N_2 adsorption isotherm, is 1098 kg m^{-3} at 77 K and 0.20 atm, which is close to the liquid O_2 density (1204 kg m^{-3}) at 77 K and 0.20 atm.

The CO_2 adsorption isotherms of SNU-50′ show CO_2 uptake capacities of 454 cm^3 g^{-1} (81 wt %) at 195 K, 120 cm^3 g^{-1} (21 wt %) at 273 K, and 80 cm^3 g^{-1} (15.7 wt %) at 298 K under 1 atm of CO_2 pressure. The highest CO_2 uptake capacities reported so far for MOFs under similar conditions is 114 wt % in SNU-6 at 195 K and 1 atm.[4a] The isosteric heat of CO_2 adsorption calculated by using the Clausius–

Clapeyron equation is 25.8 kJ mol^{-1} at low coverage range (see Figure S13 in the Supporting Information). The value is higher than that (15.8–16.5 kJ mol^{-1}) for MOF-5,[22] but similar to that of Prussian blue analogues.[23] Interestingly, the isosteric heat of adsorption only changes from 25 to 23 kJ mol^{-1} as CO_2 loading increases from 5 to 16 wt%, which indicates the strong interaction between SNU-50′ and CO_2 even at high loading.

The CH_4 uptake capacities of SNU-50′ at 1 atm are 166 cm^3 g^{-1} (12 wt%) at 195 K, 21 cm^3 g^{-1} (1.5 wt.%) at 273 K, and 17 cm^3 g^{-1} (1.2 wt%) at 298 K. The heat of CH_4 adsorption calculated by using the Clausius–Clapeyron equation is 26.8 kJ mol^{-1} at low coverage of CH_4, which indicates the strong interaction between the host framework and CH_4 gas at low coverage (see Figure S14 in the Supporting Information). The highest heat of CH_4 adsorption reported so far is 30 kJ mol^{-1} for PCN-14.[6] Contrary to CO_2 adsorption, the isosteric heat of CH_4 adsorption changes drastically from 25 to 17 kJ mol^{-1} as the loading increases from 0.5 to 1.2 wt%. The higher adsorption capacities of CO_2 relative to CH_4, and the higher isosteric heat of CO_2 adsorption (slightly depending on the amount of CO_2 loading) must be attributed to the quadrupole moment of CO_2 (1.34×10^{-39} Cm^2).

High-pressure gas-sorption properties of SNU-50′: The high-pressure gas-sorption isotherms were measured for H_2 at 77 K, and for H_2, CO_2, and CH_4 gases at 298 K (see Figure 3). SNU-50′ adsorbs an excess of 5.53 wt% H_2 at 77 K and 60 bar with no hysteresis. The total H_2 adsorption, which is the sum of the adsorbed amount on the pore surface and the amount of pressurized gas in the pore, is 7.85 wt% at 60 bar. To the best of our knowledge, only four MOFs have higher H_2 uptake capacities than this; MOF-5 (11.5 wt%, 170 bar, 77 K), MOF-177 (11.0 wt%, 70 bar, 77 K), SNU-6 (10 wt%, 50 bar, 77 K),[1] and NOTT-112 (10 wt%, 77 bar, 77 K).[24] At 298 K, the H_2 uptake capacities are reduced significantly to the excess adsorption of 0.40 wt% and the total uptake of 0.97 wt% at 60 bar.[10] NOTT-103, constructed from Cu^{II} and a long tetracarboxylate, showed a BET surface area of 2930 m^2 g^{-1} and a pore volume of 1.14 cm^3 g^{-1}.[8] It exhibited a total H_2 uptake capacity of 7.22 wt% at 77 K and 60 bar. Despite the lower BET surface area (2300 m^2 g^{-1}) and lower pore volume estimated by N_2 sorption data (1.08 cm^3 g^{-1}), SNU-50′ shows higher H_2 uptake capacity (7.85 wt%) than NOTT-103 under similar conditions, which indicates that a MOF with imide groups is better for H_2 uptake than a MOF containing simple benzene rings.

The CO_2 adsorption isotherm at 298 K also shows relatively high uptake. SNU-50′ adsorbs CO_2 with an excess adsorption of 64 wt% and a total uptake of 77 wt% at 298 K and 55 bar. The CO_2 uptake decreases slightly as the pressure increases above 45 bar, due to saturation, and the sorption isotherm shows no hysteresis. The highest CO_2 uptake capacity reported so far is 176 wt% at 304 K and 50 bar for MIL-101c(Cr).[4b]

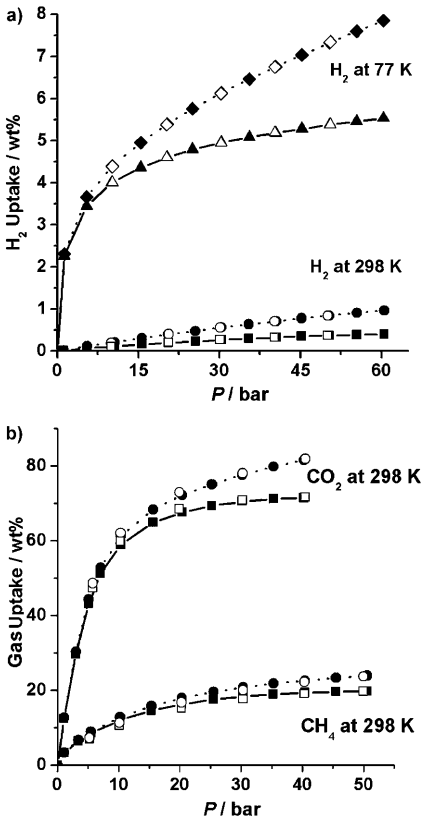

Figure 3. High-pressure gas-adsorption isotherms of SNU-50′. a) H_2 at 77 K and 298 K, b) CO_2 and CH_4 at 298 K. Solid line = excess uptake; dashed line = total uptake. Filled shape = adsorption; open shape = desorption.

SNU-50′ adsorbs CH_4 with an excess adsorption of 12 wt% and a total uptake of 17 wt% CH_4 at 298 K and 60 bar. The highest CH_4 uptake capacity reported so far is an excess adsorption of 18.1 wt% (220 v/v) with a total uptake of 18.9 wt% (230 v/v) at 35 bar and 290 K in PCN-14.[6] The high adsorption capacities for H_2 and CH_4 gases at high pressures may be attributed to the large pore volume, exposed metal sites, and the incorporation of imide groups in SNU-50′.[1,6,8]

Synthesis and X-ray crystal structure of SNU-51: Framework SNU-51 was synthesized by heating $Zn(NO_3)_2$ and H_4BDCPPI in DMF at 110 °C for 12 h, similarly to SNU-50. The X-ray crystal structure indicates that the framework structure of SNU-51 is entirely different from that of SNU-50. Instead of the paddlewheel-type SBUs in SNU-50, distorted tetrahedral $[Zn_2(OOC)_4(dmf)_3]$ SBUs are formed, and they are linked with the square-planar tetracarboxylate, which gives rise to a PtS-type network (see Figure 4). In SNU-51 there are two crystallographically independent Zn atoms, Zn1 and Zn2. They both have distorted octahedral geometry; one through coordination of six oxygen atoms of four BDCPPI^{4-} units, and the other through coordination of three carboxylate oxygen atoms and three DMF oxygen atoms. The network contains two types of rectangular chan-

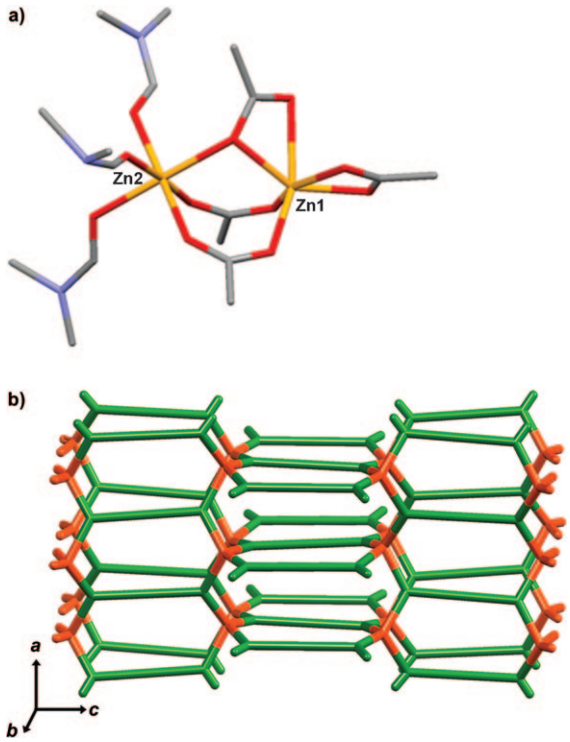

Figure 4. X-ray crystal structure of SNU-51. a) View of the $[Zn_2(OOC)_4(dmf)_3]$ SBU. b) Schematic representation of the framework: $[Zn_2(OOC)_4(dmf)_3]$ unit = orange, BDCPPI ligand = green.

nels with effective aperture sizes of 3×10 and 2×8 Å^2 along the *a* axis of the unit cell (see Figure S4 in the Supporting Information). Along the *b* axis, there are also two types of channels with effective aperture sizes of 3×13 and 2×10 Å^2. The channels running parallel to the *c* axis are completely blocked by the coordinated DMF molecules, but channels of 3 Å in diameter are generated on removal of the DMF (see Figure S4 in the Supporting Information). The guest molecules in the framework could not be determined from the difference map due to their severe thermal disorder in the large unit cell, and thus they were characterized by EA and TGA. The void volume of the framework without any guest solvent molecules is 50% of the cell volume, while the void volume increases to 69% on removal of the coordinated DMF molecules, as estimated by PLATON.[17] The measured PXRD pattern of SNU-51 is not coincident with the simulated pattern derived from the single-crystal X-ray data due to changes in the framework structure on release of the guest molecules during powder sample preparation. TGA shows that all guest molecules can be removed below 120°C, while the coordinated DMF molecules are removed slowly at 120–430°C (see Figure S6 in the Supporting Information). The desolvated framework collapses according to the PXRD pattern. The activated solid does not absorb any gas independent of the activation temperature (between 25 and 150°C under vacuum), which confirms the collapse of the framework.

Metal-ion exchange of SNU-51: The structure of SNU-51 is composed of relatively uncommon SBUs[25] and has a large crystallographic free volume. Therefore, we explored the possibility of replacing the Zn^{II} ions in SNU-51 with other metal ions, such as Cu^{II}, by a postsynthetic method; whereby crystals of SNU-51 were immersed in a 0.1 M solution of $Cu(NO_3)_2\cdot2.5H_2O$ in MeOH. The color of the crystals changed from pale yellow to green–blue in a few minutes, and then to a more intense blue over four days, as observed under an optical microscope (see Figure 5). During this process, the

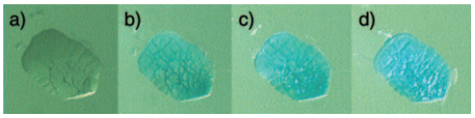

Figure 5. Photos of crystal SNU-51 taken during the exchange of Zn^{II} with Cu^{II} by immersion in a MeOH solution of $Cu(NO_3)_2$ (0.1 M) for four days. a) 0 h, b) 2 h, c) 24 h, and d) 96 h.

thin platelike crystals developed cracks and, although their transparency was retained, a single-crystal X-ray structure could not be determined for the Cu^{II} structure. Inductively coupled plasma–atomic emission spectroscopy (ICP-AES) for the resulting crystals indicated that 97% of the Zn^{II} ions had been exchanged with Cu^{II} over the four days. Interestingly, in the MeOH solution that contained the mixture of Co^{II}, Ni^{II}, Cu^{II}, and Cd^{II} ions, the Zn^{II} ions in SNU-51 were exchanged only with Cu^{II} ions. In particular, the metal exchange was very sensitive to the solvent used. For example, when DMF or 1-pentanol was used instead of MeOH, the Zn^{II} ions in SNU-51 were not exchanged with Cu^{II}, and color of the crystals did not change. In acetone, the exchange was extremely slow. This indicates that the diffusion of metal ions into the channels is sensitive to the size of the solvated metal ion and counteranion.

To prepare the metal-ion-exchanged sample on a bulk scale, SNU-51 was pulverized and stirred in a solution of 0.1 M $Cu(NO_3)_2\cdot2.5H_2O$ in MeOH for two days. The isolated powder was suspended in fresh MeOH for a further three days to remove any extra $Cu(NO_3)_2$ inclusions from the pores. The process yielded $\{[Cu_2(bdcppi)(MeOH)_3]\cdot6MeOH\cdot7H_2O\}_n$ (SNU-51-Cu_{MeOH}) as confirmed by IR, TG, and EA. The counteranion (NO_3^-) of the substituting metal ion was not detected in the IR spectra for any samples taken during the ion-exchange process. The PXRD pattern of SNU-51-Cu_{MeOH} was significantly broadened. However, when SNU-51-Cu_{MeOH} was immersed in DMF for 24–48 h, the PXRD pattern became similar to that of SNU-51 (see Figure 6). In addition, the color of SNU-51-Cu_{MeOH} changed from blue to green after immersion in DMF for a few minutes, which indicated that DMF molecules had become coordinated at the Cu^{II} ions. IR, EA, and TGA confirmed that $\{[Cu_2(bdcppi)(dmf)_3]\cdot7DMF\cdot5H_2O\}_n$ (SNU-51-Cu_{DMF}) had formed. The PXRD pattern of SNU-51-Cu_{DMF} was similar to that of SNU-51, which indicated that the framework structure was maintained during the metal ex-

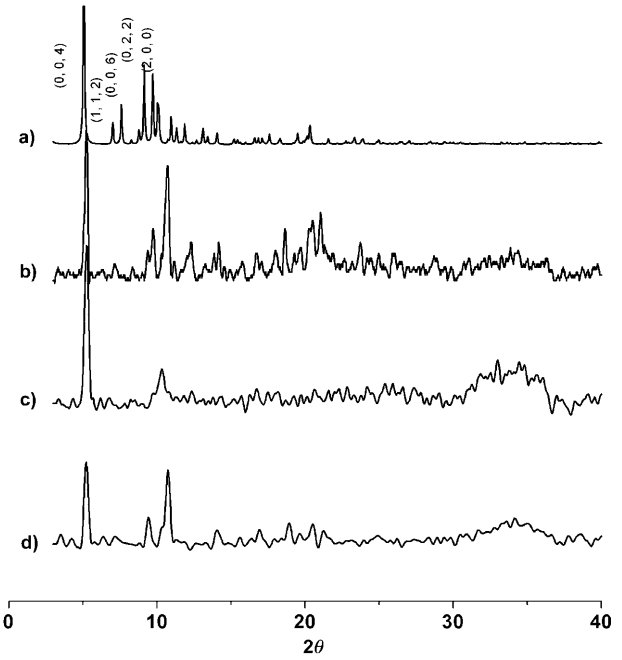

Figure 6. The PXRD patterns. a) Simulated pattern from the single crystal X-ray data of SNU-51, b) as synthesized SNU-51, c) the metal-exchanged sample, SNU-51-Cu_{MeOH}, and d) SNU-51-Cu_{DMF}.

change (see Figure 6). The Cu^{II}-exchanged sample, SNU-51-Cu_{DMF}, did not undergo ion exchange with Zn^{II} even in a concentrated solution of $Zn(NO_3)_2$ (ca. 0.1 M) in MeOH.

The kinetics of metal-ion exchange were followed by measuring the relative amount of Zn^{II} to Cu^{II} in the solid at specific time intervals. During the reaction, a small portion of the solid sample was removed and converted to SNU-51-Cu_{DMF}, and the ratio of Zn^{II} to Cu^{II} was determined by ICP-AES. The exchange of Zn^{II} with Cu^{II} was very fast during the initial stage; 27% conversion took place within 10 min, 44% within 30 min, and 75% within 2 h. Within 6 h, 97% of Zn^{II} in SNU-51 had been replaced with Cu^{II} (see Figure 7). This fast exchange process excludes the possibility of dissolution followed by recrystallization; rather, it indicates direct metal-ion exchange.

This type of metal-ion exchange is important for the preparation of new MOFs that cannot be synthesized by direct solvothermal reactions, although the mechanism is unclear at this point. The exchange described herein between Zn^{II} and Cu^{II} in a 3D MOF is unprecedented. It had been reported previously that a Cd MOF could be converted to a Pb MOF, which could then be transformed back to the Cd MOF by metal-ion exchange.[14] In that case, the Cd and Pb MOFs had the same structures and could also be synthesized by direct solvothermal reactions. In the present work, a direct solvothermal reaction of Cu^{II} with the BDCPPI ligand yielded a NbO-type net structure, whereas the reaction of Zn^{II} with the same ligand yielded a PtS-type net structure. The Cu^{II} MOF with the PtS-type net topology could be prepared only by using the postsynthetic metal-ion exchange strategy.

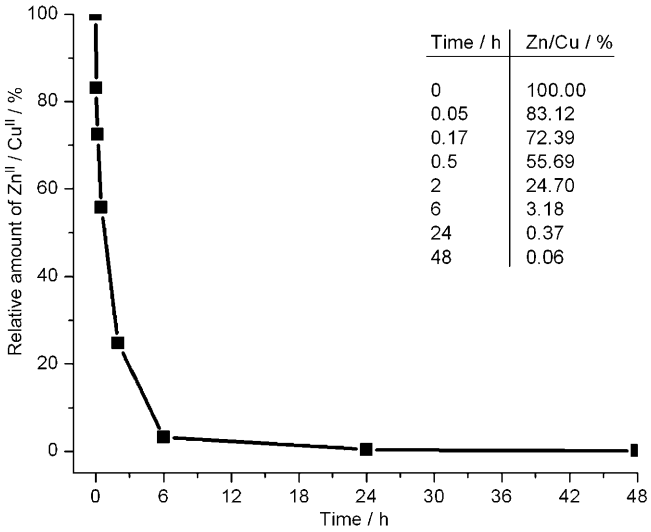

Time / h	Zn/Cu / %
0	100.00
0.05	83.12
0.17	72.39
0.5	55.69
2	24.70
6	3.18
24	0.37
48	0.06

Figure 7. Metal-ion exchange of SNU-51 with Cu^{II}. The change in the relative amount of Zn^{II} over Cu^{II} with immersion time of SNU-51 in the Cu^{II} solution. Raw data are presented in the inset table.

Conclusion

We have synthesized new porous MOFs, SNU-50 and SNU-51 by utilizing a long tetracarboxylate with imide groups, H_4BDCPPI. The desolvated solid (SNU-50′) adsorbs high levels of N_2, H_2, O_2, CO_2, and CH_4 gases due to the presence of vacant coordination sites at the metal ions, and to the presence of imide groups in the ligands. The framework adsorbs 2.10 wt% of H_2 at 1 atm and 77 K with an isosteric heat of H_2 adsorption of 7.1 kJ mol^{-1}, and a total 7.85 wt% of H_2 at 77 K and 60 bar. Of particular note is the O_2 adsorption capacity (829 cm^3 g^{-1} at 77 K and 0.20 atm), which is the highest yet reported for any MOF. The solvothermal reaction of Zn^{II} with the same ligand under similar conditions gives rise to SNU-51, with a PtS-type net that is entirely different from the NbO-type net of Cu^{II} MOF (SNU-50). Interestingly, the Zn^{II} ions in SNU-51 could be exchanged with Cu^{II} ions to afford the Cu^{II} MOF with a PtS-type net, which could not be produced from direct solvothermal synthesis. This result suggests that the metal-ion-exchange strategy can be utilized for the synthesis of new MOFs that cannot otherwise be obtained by direct solvothermal reactions.

Experimental Section

Ligand synthesis: The synthesis of *N,N′*-bis(3,5-dicarboxyphenyl)pyromellitic diimide (H_4BDCPPI) was achieved by using a modified version of a previously reported procedure:[26] 1,2,4,5-benzene tetracarboxylate dianhydride (2.18 g, 10 mmol) and 5-aminoisophthalic acid (3.62 g, 20 mmol) were dissolved in DMF (40 mL). The solution was heated at reflux for 8 h, and then allowed to cool to room temperature. A pale yellow crystalline precipitate (2.80 g, 51%) was formed, which was filtered, washed with MeOH, and dried under vacuum. ^{1}H NMR (300 MHz, [D_6]DMSO, 25 °C): δ = 8.36 (s; 4H), 8.43 (s; 2H), 8.55 ppm (s; 2H); IR (KBr): $\tilde{\nu}$ =

1777, 1732 (C=O(pyromellitic diimide)), 1660, 1601 cm^{-1} (C=O(carboxylic acid)); elemental analysis calcd (%) for $C_{26}H_{12}N_2O_{12}{\cdot}0.5C_3H_7NO$: C 56.85, H 2.69, N 6.02; found: C 55.78, H 2.83, N 5.93.

Preparation of $\{[Cu_2(bdcppi)(dmf)_2]\cdot 10\,DMF\cdot 2H_2O\}_n$ (SNU-50): $Cu(NO_3)_2{\cdot}2.5H_2O$ (0.024 g, 0.103 mmol), H_4BDCPPI (0.030 g, 0.051 mmol), and DMF (5 mL) were placed in a glass bottle, and acidified with HNO_3 (13 N, 3 drops). The bottle was sealed and heated at 110 °C for 12 h. Blue–green prismatic crystals (0.045 g, 60 %) formed, which were filtered and washed with DMF. IR (KBr): $\tilde{\nu}$ = 1780, 1728 (C=O(pyromellitic diimide)), 1667 (C=O(coordinated DMF)), 1640 (sh), 1590 cm^{-1} (carboxylate); UV/Vis (diffuse reflectance): λ_{max} = 760, 715 nm; elemental analysis calcd (%) for $C_{62}H_{96}Cu_2N_{14}O_{26}$: C 47.11, H 6.12, N 12.41; found: C 46.92, H 6.35, N 12.79.

Preparation of $\{[Cu_2(bdcppi)(CH_3COCH_3)_2]\cdot 5\,CH_3COCH_3\cdot 2H_2O\}_n$ ($SNU\text{-}50_{Ac}$): Crystals of SNU-50 were immersed in dried acetone for 5–7 days. The acetone was removed by decanting, and was replaced with fresh acetone at least twice a day. The color of the crystals changed from blue–green to gray–blue. IR (nujol): $\tilde{\nu}$ = 1781, 1729 (C=O(pyromellitic diimide)), 1703 (C=O(guest acetone)), 1689 (m, C=O(coordinated acetone)), 1637, 1591 cm^{-1} (carboxylate); UV/Vis (diffuse reflectance): λ_{max} = 690 nm; elemental analysis calcd (%) for $C_{47}H_{54}Cu_2N_2O_{21}$: C 50.85, H 4.90, N 2.52; found: C 50.66, H 4.65, N 2.66.

Preparation of $[Cu_2(bdcppi)]_n$ (SNU-50′): Crystals of $SNU\text{-}50_{Ac}$ (≈0.2 g) were transferred to a gas adsorption cell and the cell was kept under N_2 flow at room temperature for 30 min to remove loosely bound solvent molecules. The sample was activated on the gas sorption instrument at 60 °C for 24 h and then at 170 °C for 4 h under vacuum. The color of the crystals changed from gray–blue to dark purple–blue (the color of the activated compound instantly changes to pale green upon exposure to air). IR (nujol; prepared under Ar in glove bag): $\tilde{\nu}$ = 1782, 1735 (C=O(pyromellitic diimide)), 1630, 1588 cm^{-1} (carboxylate); elemental analysis calcd (%) for $C_{26}H_8Cu_2N_2O_{12}$: C 46.79, H 1.21, N 4.20; found: C 46.86, H 1.23, N 4.46.

Preparation of $\{[Zn_2(bdcppi)(dmf)_3]\cdot 6\,DMF\cdot 4H_2O\}_n$ (SNU-51): $Zn(NO_3)_2{\cdot}6H_2O$ (0.029 g, 0.100 mmol), H_4BDCPPI (0.030 g, 0.051 mmol), and DMF (5 mL) were placed in a glass bottle, which was sealed with rubber and aluminum caps and heated at 110 °C for 12 h. On cooling to room temperature, yellow platelike crystals formed (0.040 g, 57 %), which were filtered and washed with DMF. IR (KBr): $\tilde{\nu}$ = 1779, 1727 (C=O(pyromellitic diimide)), 1668 (C=O(coordinated DMF)), 1632 (sh), 1587 cm^{-1} (carboxylate); elemental analysis calcd (%) for $C_{53}H_{79}Zn_2N_{11}O_{25}$: C 45.43, H 5.68, N 11.00; found: C 44.24, H 5.25, N 11.07.

Preparation of $\{[Cu_2(bdcppi)(MeOH)_3]\cdot 6\,MeOH\cdot 7H_2O\}_n$ ($SNU\text{-}51\text{-}Cu_{MeOH}$): Crystals of SNU-51 (≈0.75 g) were pulverized and added to a solution of $Cu(NO_3)_2{\cdot}2.5H_2O$ (0.1 M, 100 mL) in methanol, which was then stirred for 48 h. The color of the solid changed from pale yellow to blue. After 6 h and then 24 h of immersion, the $Cu(NO_3)_2$ solution was removed by decanting, and replenished with fresh $Cu(NO_3)_2$ solution in methanol. The compound was isolated and suspended in fresh MeOH for three days at 50 °C to remove any Cu or Zn salt present in the pores of the framework. During this process, the MeOH was removed by decanting, and was replaced with fresh MeOH at least twice. IR (KBr): $\tilde{\nu}$ = 1782, 1727 (C=O(pyromellitic diimide)), 1652, 1630 (sh), 1563 cm^{-1} (carboxylate); elemental analysis calcd (%) for $Cu_2C_{35}H_{58}N_2O_{28}$: C 38.85, H 5.40, N 2.59; found: C 38.58, H 5.13, N 2.61.

Preparation of $\{[Cu_2(bdcppi)(dmf)_3]\cdot 7\,DMF\cdot 5H_2O\}_n$ ($SNU\text{-}51\text{-}Cu_{DMF}$): A suspension of $SNU\text{-}51\text{-}Cu_{MeOH}$ in methanol was decanted to remove the methanol, and DMF was added, during which time the color of the solid changed to blue–green. The solid was kept in DMF for three days, which afforded $SNU\text{-}51\text{-}Cu_{DMF}$. IR (KBr): $\tilde{\nu}$ = 1782, 1728 (C=O(pyromellitic diimide)), 1663 (C=O(coordinated DMF)), 1630 (sh), 1591 (m), 1560 cm^{-1} (m; carboxylate); UV/Vis (diffuse reflectance): λ_{max} = 810, 770, 670 nm; elemental analysis calcd (%) for $Cu_2C_{56}H_{88}N_{12}O_{27}$: C 45.19, H 5.96, N 11.29; found: C 45.30, H 6.02, N 11.29.

Kinetics of metal-ion exchange: The pulverized crystals of SNU-51 were immersed in a solution of $Cu(NO_3)_2{\cdot}2.5H_2O$ in MeOH. A small amount of solid sample was removed at specific time intervals and suspended in DMF. The $SNU\text{-}51\text{-}Cu_{DMF}$ was decomposed with concentrated HNO_3, and the ratio of Zn/Cu was determined by ICP-AES.

Selective metal-ion exchange experiment: Crystals of SNU-51 were immersed in a mixture of $Co(NO_3)_2{\cdot}6H_2O$, $Ni(NO_3)_2{\cdot}6H_2O$, $Cu(NO_3)_2{\cdot}2.5H_2O$, and $Cd(NO_3)_2{\cdot}6H_2O$ (0.1 M, 15 mL). The crystals were isolated from the solution after 24 h, and suspended in fresh MeOH for three days. The crystals were filtered and decomposed with concentrated HNO_3. ICP-AES analysis gave the following composition: 77.4 % Cu, 18.3 % Zn, 1.2 % Co, 1.3 % Ni, and 1.9 % Cd, which indicated that metal exchange was selective.

X-ray crystallography: Data were collected on an Enraf Nonius Kappa CCD diffractometer by using graphite-monochromated $Mo_{K\alpha}$ radiation (λ = 0.71073 Å) at 298 K. Each crystal was sealed in a glass capillary together with the mother liquor. Preliminary orientation matrices and unit cell parameters were obtained from the peaks of the first ten frames and then refined with the whole data set. Frames were integrated and corrected for Lorentz and polarization effects by using DENZO.[27] Scaling and global refinement of crystal parameters were performed by using SCALEPACK.[27] The structure was solved by using SHELXS-97.[28] All hydrogen atoms were assigned on the basis of geometrical considerations and allowed to ride on the respective carbon atoms. The solvent molecules could not be located from the difference maps, and the residual electron density corresponding to the solvent molecules were ignored by using the SQUEEZE[29] option of PLATON.[17] Because of the disorder in the benzene rings, all atoms except Cu and O in SNU-50 were refined isotropically. CCDC-760674 and 760675 contain the supplementary crystallographic data for this paper. These data can be obtained free of charge from The Cambridge Crystallographic Data Centre via www.ccdc.cam.ac.uk/data_request/cif. Crystallographic data for SNU-50 and SNU-51 are summarized in Table 2.

Table 2. Crystallographic data for SNU-50 and SNU-51 (squeezed data).

	SNU-50	SNU-51
formula	$C_{32}H_{22}Cu_2N_4O_{14}$	$C_{35}H_{29}N_5O_{15}Zn_2$
space group	R_{-3m}	*Icab*
M_r	813.64	890.41
a [Å]	18.794(7)	18.119(3)
b [Å]	18.794(7)	20.125(4)
c [Å]	50.17(2)	69.8204(14)
α [°]	90	90
β [°]	90	90
γ [°]	120	90
V [Å^3]	15347(10)	25572(7)
Z	9	16
ρ_{calcd} [g cm^{-3}]	0.792	0.925
T [K]	298	298
μ [mm^{-1}]	0.661	0.796
GOF (F^2)	0.846	1.040
R_1,wR_2 [$I > 2\sigma(I)$]	0.1049,[a] 0.2698[b]	0.0817,[a] 0.2293[c]
R_1,wR_2 (all data)	0.2099,[a] 0.3113[b]	0.1277,[a] 0.2419[c]

[a] $R = \Sigma||F_0| - |F_c||/\Sigma|F_0|$. [b] $wR(F^2) = [\Sigma w(F_0^2 - F_c^2)^2/\Sigma w(F_0^2)^2]^{1/2}$ in which $w = 1/[\sigma^2(F_0^2) + (0.1582P)^2 + (0.0000)P]$, $P = (F_0^2 + 2F_c^2)/3$ for SNU-50. [c] $wR(F^2) = [\Sigma w(F_0^2 - F_c^2)^2/\Sigma w(F_0^2)^2]^{1/2}$ in which $w = 1/[\sigma^2(F_0^2) + (0.1146P)^2 + (0.0000)P]$, $P = (F_0^2 + 2F_c^2)/3$ for SNU-51.

Gas sorption measurements: Low-pressure gas adsorption–desorption measurements were performed by using Autosorb-1 or Autosorb-3B (Quantachrome Instruments). All gases used were of 99.999 % purity. After gas sorption measurements, the sample was precisely weighed again. The surface area and total pore volume were determined from the N_2 gas isotherm at 77 K. For multipoint BET and Langmuir surface area estimations, the data were taken in the range of P/P_0 = 0.001–0.08 and P/P_0 = 0.0001–0.016, respectively. High-pressure gas sorption isotherms of SNU-50′ were measured for H_2 (77 K), CO_2 (298 K), and CH_4 (298 K) in the range 1–60 bar by the gravimetric method with a Rubotherm magnetic suspension balance (MSB). Crystals of $SNU\text{-}50_{Ac}$ were heated at 60 °C

for 3 h and 170 °C for 20 h with gas sorption apparatus under vacuum. All data were corrected for buoyancy of the system and sample. The sample density used in the buoyancy correction was determined from He displacement isotherms measured at 298 K.

Acknowledgements

This work was supported by National Research Foundation of Korea (NRF) Grant funded by the Korean Government (MEST) (no. 2009-0093842 and no. 2010-0001485).

[1] L. J. Murray, M. Dinca, J. R. Long, *Chem. Soc. Rev.* **2009**, *38*, 1294–1314.
[2] a) J.-R. Li, R. J. Kuppler, H.-C. Zhou, *Chem. Soc. Rev.* **2009**, *38*, 1477–1504; b) M. P. Suh, Y. E. Cheon, E. Y. Lee, *Coord. Chem. Rev.* **2008**, *252*, 1007–1026; c) J. Lee, O. K. Farha, J. Roberts, K. A. Scheidt, S. T. Nguyen, J. T. Hupp, *Chem. Soc. Rev.* **2009**, *38*, 1450–1459; d) L. Q. Ma, C. Abney, W. B. Lin, *Chem. Soc. Rev.* **2009**, *38*, 1248–1256; e) M. P. Suh, H. R. Moon, E. Y. Lee, S. Y. Jang, *J. Am. Chem. Soc.* **2006**, *128*, 4710–4718; f) Y. E. Cheon, M. P. Suh, *Angew. Chem.* **2009**, *121*, 2943–2947; *Angew. Chem. Int. Ed.* **2009**, *48*, 2899–2903.
[3] Y. G. Lee, H. R. Moon, Y. E. Cheon, M. P. Suh, *Angew. Chem.* **2008**, *120*, 7855–7859; *Angew. Chem. Int. Ed.* **2008**, *47*, 7741–7745.
[4] a) H. J. Park, M. P. Suh, *Chem. Eur. J.* **2008**, *14*, 8812–8821; b) P. L. Llewellyn, S. Bourrelly, C. Serre, A. Vimont, M. Daturi, L. Hamon, G. De Weireld, J.-S. Chang, D.-Y. Hong, Y. K. Hwang, S. H. Jhung, G. Ferey, *Langmuir* **2008**, *24*, 7245–7250; c) A. R. Millward, O. M. Yaghi, *J. Am. Chem. Soc.* **2005**, *127*, 17998–17999; d) H.-S. Choi, M. P. Suh, *Angew. Chem.* **2009**, *121*, 6997–7001; *Angew. Chem. Int. Ed.* **2009**, *48*, 6865–6869.
[5] X.-S. Wang, S. Q. Ma, K. Rauch, J. M. Simmons, D. Q. Yuan, X. P. Wang, T. Yildirim, W. C. Cole, J. J. Lopez, A. de Meijere, H.-C. Zhou, *Chem. Mater.* **2008**, *20*, 3145–3152.
[6] S. Q. Ma, D. F. Sun, J. M. Simmons, C. D. Collier, D. Q. Yuan, H.-C. Zhou, *J. Am. Chem. Soc.* **2008**, *130*, 1012–1016.
[7] H. Wu, W. Zhou, T. Yildirim, *J. Am. Chem. Soc.* **2009**, *131*, 4995–5000.
[8] X. Lin, I. Telepeni, A. J. Blake, A. Dailly, C. M. Brown, J. M. Simmons, M. Zoppi, G. S. Walker, K. M. Thomas, T. J. Mays, P. Hubberstey, N. R. Champness, M. Schroder, *J. Am. Chem. Soc.* **2009**, *131*, 2159–2171.
[9] a) H. Furukawa, M. A. Miller, O. M. Yaghi, *J. Mater. Chem.* **2007**, *17*, 3197–3204; b) A. G. Wong-Foy, A. J. Matzger, O. M. Yaghi, *J. Am. Chem. Soc.* **2006**, *128*, 3494–3495; c) A. G. Wong-Foy, O. Lebel, A. J. Matzger, *J. Am. Chem. Soc.* **2007**, *129*, 15740–15741.
[10] a) S. S. Kaye, A. Dailly, O. M. Yaghi, J. R. Long, *J. Am. Chem. Soc.* **2007**, *129*, 14176–14177; b) M. Dinca, A. Dailly, Y. Liu, C. M. Brown, D. A. Neumann, J. R. Long, *J. Am. Chem. Soc.* **2006**, *128*, 16876–16883.
[11] S. H. Yang, X. Lin, A. Dailly, A. J. Blake, P. Hubberstey, N. R. Champness, M. Schroder, *Chem. Eur. J.* **2009**, *15*, 4829–4835.
[12] a) X. Lin, J. H. Jia, X. B. Zhao, K. M. Thomas, A. J. Blake, G. S. Walker, N. R. Champness, P. Hubberstey, M. Schroder, *Angew. Chem.* **2006**, *118*, 7518–7524; *Angew. Chem. Int. Ed.* **2006**, *45*, 7358–7364; b) X.-S. Wang, S. Q. Ma, P. M. Forster, D. Q. Yuan, J. Eckert, J. J. Lopez, B. J. Murphy, J. B. Parise, H.-C. Zhou, *Angew. Chem.* **2008**, *120*, 7373–7376; *Angew. Chem. Int. Ed.* **2008**, *47*, 7263–7266; c) M. Xue, G. S. Zhu, Y. X. Li, X. J. Zhao, Z. Jin, E. Kang, S. L. Qiu, *Cryst. Growth Des.* **2008**, *8*, 2478–2483; d) A. J. Cairns, J. A. Perman, L. Wojtas, V. C. Kravtsov, M. H. Alkordi, M. Eddaoudi, M. J. Zaworotko, *J. Am. Chem. Soc.* **2008**, *130*, 1560–1561.
[13] a) Z. Q. Wang, S. M. Cohen, *Chem. Soc. Rev.* **2009**, *38*, 1315–1329; b) T. Uemura, N. Yanai, S. Kitagawa, *Chem. Soc. Rev.* **2009**, *38*, 1228–1236.
[14] S. Das, H. Kim, K. Kim, *J. Am. Chem. Soc.* **2009**, *131*, 3814–3815.
[15] a) T. Akitsu, Y. Einaga, *Acta Crystallogr. Sect. C* **2004**, *60*, m162–m164; b) D. A. Grossie, W. A. Feld, L. Scanlon, G. Sandi, Z. Wawrzak, *Acta Crystallogr. Sect. E* **2006**, *62*, m827–m829.
[16] T. Duren, F. Millange, G. Férey, K. S. Walton, R. Q. Snurr, *J. Phys. Chem. C* **2007**, *111*, 15350–15356.
[17] a) A. L. Spek, *Acta Crystallogr. Sect. A* **1990**, *46*, C34; b) A. L. Spek, PLATON, A Multipurpose Crystallographic Tool, Utrecht University, Utrecht, **1998**.
[18] A. Saito, H. C. Foley, *AIChE J.* **1991**, *37*, 429–436.
[19] a) L. Czepirski, J. Jagiello, *Chem. Eng. Sci.* **1989**, *44*, 797–801; b) J. L. C. Rowsell, O. M. Yaghi, *J. Am. Chem. Soc.* **2006**, *128*, 1304–1315.
[20] H. J. Choi, M. Dinca, J. R. Long, *J. Am. Chem. Soc.* **2008**, *130*, 7848–7850.
[21] Y. Li, R. T. Yang, *Langmuir* **2007**, *23*, 12937–12944.
[22] J.-S. Choi, W.-J. Son, J. Kim, W.-S. Ahn, *Microporous Mesoporous Mater.* **2008**, *116*, 727–731.
[23] S. Natesakhawat, J. T. Culp, C. Matranga, B. Bockrath, *J. Phys. Chem. C* **2007**, *111*, 1055–1060.
[24] Y. Yan, X. Lin, S. H. Yang, A. J. Blake, A. Dailly, N. R. Champness, P. Hubberstey, M. Schroder, *Chem. Commun.* **2009**, 1025–1027.
[25] B. L. Chen, N. W. Ockwig, F. R. Fronczek, D. S. Contreras, O. M. Yaghi, *Inorg. Chem.* **2005**, *44*, 181–183.
[26] C. Degenhardt III, D. B. Shortell, R. D. Adams, K. D. Shimizu, *Chem. Commun.* **2000**, 929–930.
[27] DENZO-SCALEPACK: Z. Otwinowski, W. Minor, *Processing of X-ray Diffraction Data Collected in Oscillation Mode, Methods in Enzymology, Vol. 276: Macromolecular Crystallography, Part A* (Eds.: C. W. Carter, Jr., R. M. Sweet), Academic Press, New York, **1997**, pp. 307–326.
[28] G. M. Sheldrick, SHELXS-97: Programs for crystal structure analysis, University of Göttingen, Göttingen (Germany), **1997**.
[29] P. van der Sluis, A. L. Spek, *Acta Crystallogr. Sect. A* **1990**, *46*, 194–201.

Received: July 26, 2010
Published online: October 22, 2010

